"Shaking in 5 seconds!" A Voluntary Smartphone-based Earthquake Early Warning System

Rémy Bossu[1], Francesco Finazzi[2], Robert Steed[1], Laure Fallou[1], and István Bondár[3]

[1]EMSC-CSEM
[2]University of Bergamo
[3]Research Center for Astronomy and Earth Sciences

November 24, 2022

Abstract

Public earthquake early warning systems have the potential to reduce individual risk by warning people of an incoming tremor, but their development is hampered by costly infrastructure. Furthermore, users' understanding of such a service and their reactions to warnings remains poorly studied. The Earthquake Network app turns users' smartphones into motion detectors and provides rapid information about felt earthquakes in multiple countries. It offers an alternative without the need of dedicated infrastructure in the many regions unlikely to be covered by conventional early warning systems in the foreseeable future. We show here that it already provides an early warning service, including for damaging shaking levels and although warnings are appreciated and understood by users, only a fraction follow the "drop, cover and hold" advice.

"Shaking in 5 seconds!" A Voluntary Smartphone-based Earthquake Early Warning System

Rémy Bossu[1,2], Francesco Finazzi[3], Robert Steed[1], Laure Fallou[1], István Bondár[4]

[1]European-Mediterranean Seismological Centre; Arpajon, France.

[2]CEA, DAM, DIF, 91297; Arpajon, France.

[3]University of Bergamo, Department of Management, Information and Production Engineering; Dalmine, Italy.

[4] ELKH Research Centre for Astronomy and Earth Sciences, Geodetic and Geophysical Institute; Budapest, Hungary.

Corresponding author: Francesco Finazzi (francesco.finazzi@unibg.it)

Key Points:

- A study has been carried out on the performance of the first operational smartphone-based public earthquake early warning system.
- The system has been capable of providing early warning to people who experienced up to intensity 6 shaking.
- Results from a survey suggest that a small fraction of people who receive the warning take protective actions but most appreciate it.

Abstract

Public earthquake early warning systems have the potential to reduce individual risk by warning people of an incoming tremor, but their development is hampered by costly infrastructure. Furthermore, users' understanding of such a service and their reactions to warnings remains poorly studied. The Earthquake Network app turns users' smartphones into motion detectors and provides rapid information about felt earthquakes in multiple countries. It offers an alternative without the need of dedicated infrastructure in the many regions unlikely to be covered by conventional early warning systems in the foreseeable future. We show here that it already provides an early warning service, including for damaging shaking levels and although warnings are appreciated and understood by users, only a fraction follow the "drop, cover and hold" advice.

Plain language summary

Earthquake early warning systems have huge potential to mitigate the risk posed by earthquakes by issuing a timely warning of incoming earthquake tremors. However, deploying such systems requires prohibitively expensive infrastructure. The Earthquake Network app utilizes users' charging smartphones as motion detectors for seismic waves and provides rapid alerts of felt earthquakes in many countries worldwide. Being a smartphone-based volunteer network, it doesn't need dedicated infrastructure. Hence, it presents an alternative solution for many regions in the world that are unlikely to be served by traditional early warning systems in the foreseeable future. With nearly a million active users globally, it already provides an early warning service for felt and damaging shaking levels. We show that its performance and reliability in earthquake detection and warning time is comparable to conventional early warning systems. We studied users' understanding and reactions to the warning message following a magnitude 8 earthquake in Peru. Results show that users appreciate early warnings even though they don't always follow the "drop cover and hold" advice, leaving room for improvement for better communication and more effective risk mitigation.

1 Introduction

Public earthquake early warning (PEEW) systems aim to warn people of imminent shaking through the rapid detection of earthquakes. They strive to reduce an individual's risk by allowing their users to take protective actions (such as "drop, cover and hold") in the seconds or tens of seconds separating the warning from ground shaking at the user's location. They were deployed first in 1991 in Mexico City (Suárez et al., 2009) and then in Japan in 2007 (Nakayachi et al., 2019). Despite this desirable goal and the existence of a number of other implementations, such as ShakeAlert® in the Western US (Kohler et al., 2018) and some private initiatives in Mexico and Chile, so far PEEW systems have not been put into service more widely, even in regions of high earthquake hazard, because they require dense, real time, and robust seismic and communication networks (Cremen & Galasso, 2020). Furthermore, PEEW evaluations have mainly focused on technical performance (e.g., rapidity, false/missed alert rates) with only a few studies carried out from users' perspectives to assess how the service is valued and, more importantly, whether users react or not after receiving the warning (Nakayachi et al., 2019). This situation has led to a lack of actual assessment of PEEW in terms of individual risk reduction so that key parameters such as the public's tolerance to false and missed alerts remain unknown,

making it difficult to develop informed and efficient warning strategies (Allen & Melgar, 2019; Cochran & Husker, 2019).

The Earthquake Network (EQN) app is a smartphone-based PEEW system that detects earthquakes in real time by turning users' smartphones into motion monitoring stations and publishes the earthquake warnings that the network generates (Finazzi, 2020). The resulting monitoring network is fully dynamic, with new users often joining after felt earthquakes and some leaving. EQN, available in 8 languages, has grown its userbase since its inception in 2012 with 6.5 million downloads and 650,000 active users in 2020 but this is its first actual evaluation in terms of early warning. The objectives of this work are to 1) evaluate EQN's detection performance, 2) demonstrate that it is capable of providing public earthquake early warning in multiple countries, and 3) assess the potential of EQN's contribution to individual risk reduction by studying EQN users' reactions after an actual early warning. Performance has been evaluated over a 26-month period (Dec. 15th, 2017 to Jan. 31st, 2020) during which the EQN data processing methodology was not modified. In addition, reaction to and understanding of early warning by EQN users has been inferred from an online survey of local EQN users in the felt area of the M8 2019 Peru earthquake.

2 EQN's operation and alerting strategy

Installation of the EQN app turns participants' smartphones into real time seismic detectors by monitoring their internal accelerometers while their phones are charging. Hereafter, a trigger will describe the motion detection performed by a single smartphone while detection will refer to the EQN system detecting an earthquake through a statistical analysis of the collected individual triggers.

When an active (i.e., charging) smartphone senses an acceleration above a noise-dependent threshold, a smartphone trigger is sent to the EQN servers and time stamped at reception. No attempt is made to analyze seismic waveforms. A detection occurs when concurrent triggers within 30 km of each other exceed a dynamic threshold that is a function of the actual number of active smartphones and of the desired false alarm probability, a level currently set to one per year per country (Finazzi & Fassò, 2017). A geo-located alert is issued at detection time to all users within 300 km of the detection location which is the average location of those triggering smartphones and is taken as a proxy for the epicentral location. The alert is a smartphone notification with an easily recognizable sound and an automatic display of the epicentral location proxy, as well as a countdown in seconds to the estimated S-wave arrival time at the user location (see Figure S1 of Supplementary Material). Large earthquakes can cause several detections. To avoid multiple alerts for the same users only detections at least 300 km and 120 s apart are released.

Users are invited after the alert to manually report the local level of shaking through a qualitative felt report with 3 levels ("mild", "strong" or "very strong"). This is intended to identify larger earthquakes as EQN does not provide magnitude estimates. If at least 10% of the users in the area of detection submit reports and 80% of these reports are "strong" or "very strong", a second alert is issued - typically 30 s after the first one - to users in an enlarged region (600 km by default). During the studied period, no second alert was issued for magnitudes lower than 4.3 and 14 out of the 17 alerts were for magnitudes greater than 5. So, the second alert successfully excludes small earthquakes rather than identifying large ones. Users can opt in or out of the two alerts and customize alerting distances.

3 EQN detection performance

EQN detection performance in terms of latency, false detection rate and missed earthquake detections has been evaluated using the 550 detections (Steed et al., 2021a) from the 3 countries (Chile, USA, and Italy) with at least 10 detections whose national catalogues possess both good location accuracy and coverage of low magnitude earthquakes, and where accelerometric data is available. Accurate locations are required to make proper estimates of the system's latency. Catalogues including low magnitude earthquakes are essential for both network sensitivity and false detection rate estimates as smartphone detections are possible down at least to M2 (Kong et al., 2019). Finally, accelerometric data was sought out from stations close to each detection location for a final consistency check against waveform data (Steed et al., 2021b).

EQN detections were first associated in time and space with hypocenters from national catalogues, then among the potential candidates, an earthquake was considered as the source of the detection if the theoretical arrival time of the P-wave at the detection location was between 90 s before to 10 s after the detection time to consider potential transmission delay and location uncertainties. This led to an initial association of 535 out of 550 detections. For this analysis, whenever an accelerometric station was available within 20 km of the detection location (410 out of 550 detections), existence and time consistency of ground motion was visually checked. This inspection allowed the association of 4 additional detections. One was associated to a M3.8 earthquake at an unusually large distance of 350 km, and 2 to small magnitude earthquakes (M1.4 and M1.5 located 2 and 8 km from the detection) located through additional investigation by the Seismological Centre of the University of Chile. The fourth was found to be a secondary detection 800 km from epicenter of the March 1st, 2019 Peru M7.0 earthquake. The false detection rate was ~2%.

The 539 associated detections are consistent with previous detectability studies of smartphone sensors (Kong et al., 2019). With half of them related to earthquakes below M4 (Figure 1), EQN detections also include events that are unlikely to generate strong shaking and then for which an early warning may not be necessary. However, comparison with independent data (Figure 1) indicates that nearly all EQN detections are likely to have also been felt which make them relevant for rapid public information, even the few very low magnitude ones.

Assessment of EQN's rate of missed earthquakes is more complex than for traditional seismic monitoring networks as EQN geometry is governed by spatiotemporal variations in population distribution - higher in cities, lower in low population areas - and it constantly changes with app installations and deletions, and the number of active smartphones. Hence EQN detectability generally increases at night when more phones are charging. The rate of EQN earthquake detections was 3.1 times higher at night than during the day (Table 1). In Italy where the number of app users remained stable during the studied period (about 45,000) both earthquakes M≥4.9 were detected as well as 4 out of 6 earthquakes M≥4.5.

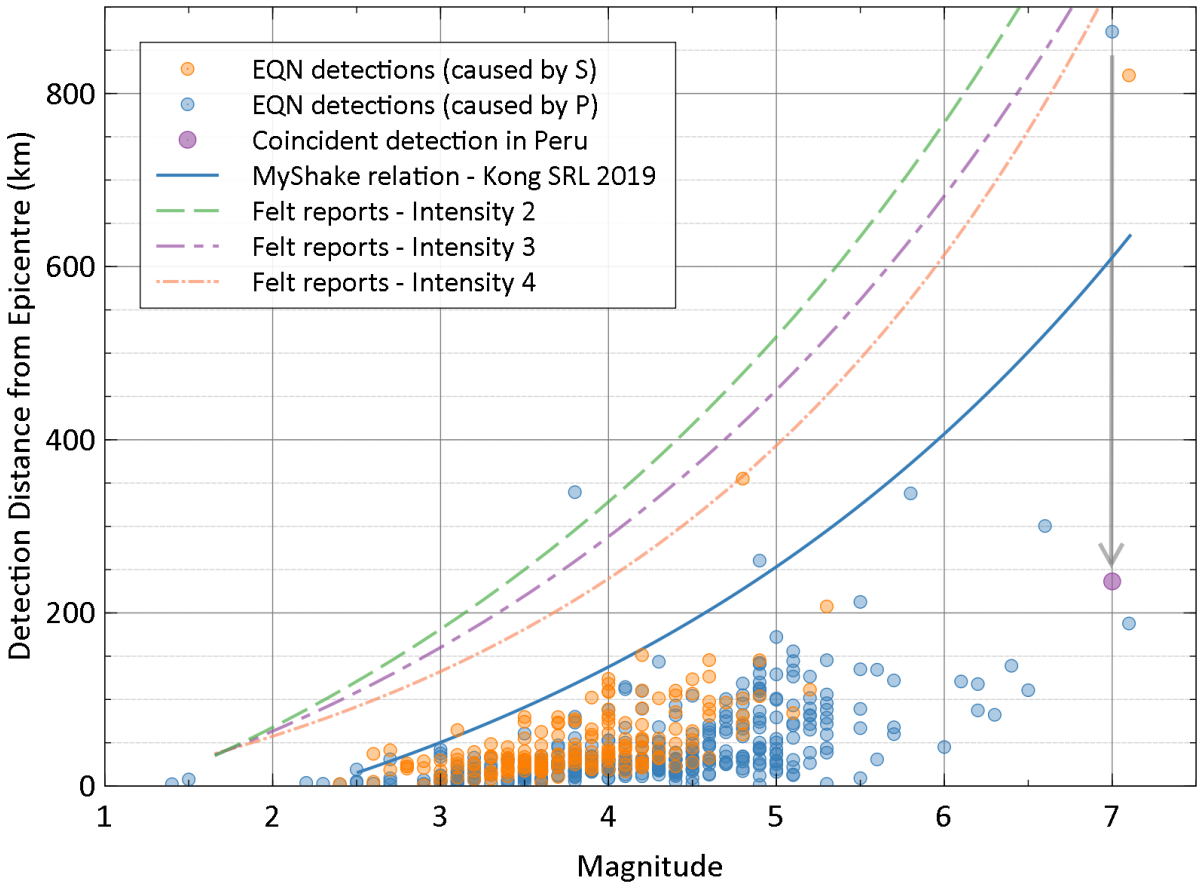

Figure 1. Distance between the location of the detection and the epicenter distance for 539 EQN associated detections as a function of magnitude. Blue and orange dots represent detections likely caused by P and S waves, respectively (the causative seismic phase is uncertain for epicentral distances below about 50 km, see Supplementary Material). The M7 earthquake detected at more than 800 km epicentral distance was also detected in Peru, at about 250 km epicentral distance (arrow and purple dot). For comparison, the blue curve approximates the maximum distance to which smartphones operating MyShake app can detect earthquakes (Kong et al., 2019) while the 3 dashed lines approximate the 90% radial distance quantile of user-assigned intensities 2 (scarcely felt), 3 (weak) and 4 (largely observed) (based on the 1,528 global earthquakes between 2011 and end of October 2020 with at least 100 felt reports collected by the European-Mediterranean Seismological Center (EMSC).

164 **Table 1**. *Summary statistics of EQN detections in Chile, USA, and Italy.*
165

Country	Chile	USA	Italy	Total
Detections	458	70	22	550
Detections associated with known earthquakes	449	70	20	539
Available accelerometric records	328	69	13	410
Magnitude (min; max)	1.4; 7.1	2.2; 7.1	2.4; 5.1	1.4; 7.1
Detection delay (in s) w.r.t. origin time (min; median; max)	4.8; 17.2; 209.0	4.3; 8.1; 42.5	3.4; 7.3; 11.0	3.4; 15.4; 209.0
Detection delay (in s) w.r.t. passing of triggering seismic wave (min; median; max)	0.5; 4.3; 12.1	2.0; 4.6; 10.2	1.8; 4.5; 5.9	0.5; 4.3; 12.1
False detection rate (%)	2.0	0.0	9.1	2.0
Nighttime/daytime ratio	2.7	11.3	8.0	3.1
Source of catalogue	CSN	USGS	INGV	

166 *Note*: Associated detections are the number of EQN detections for which it was possible to
167 identify the causative earthquake. The accelerometric record column gives the number of
168 detections for which accelerometric data is available within 20 km of the detection location.
169 Detection delays are computed with respect to the earthquake origin time and the most likely
170 causative seismic phase. False detection rate is the ratio between the number of false detections
171 and the total number of detections while the nighttime/daytime ratio is computed considering
172 that day (7:00 a.m. - 10:59 p.m.) lasts twice the night. CSN: Centro Sismologico Nacional, Chile.
173 INGV: Istituto Nazionale Geologia e Vulcanologia, Italy.

174 **4 Latency of earthquake detections from a dynamic monitoring network**

175 The shortest earthquake detection latencies, i.e., the time difference between earthquake origin
176 time and alert issuance, are achieved when the hypocenter is close to regions where the EQN app
177 is popular. This explains why the median detection time was around 7-8 s in Italy and USA,
178 where all detected earthquakes were onshore and at crustal depth (<40 km) compared to 17 s in
179 Chile where a significant proportion of detected earthquakes were offshore and/or at intermediate
180 depth (Table 1).

A limited comparison of earthquake detection times can be performed with ShakeAlert®, the operational EEW system which aims to cover the West Coast of the USA with 1,700 seismic stations (Kohler et al., 2018). Four earthquakes, the M7.1 Ridgecrest mainshock and 3 of its aftershocks ranging in magnitude from 3.8 to 4.5 were detected by both systems. Excluding the case of the mainshock discussed below, EQN latencies are larger by an average 1.6 s (7.6 s versus 6.0 s averages for EQN and ShakeAlert® respectively) which is rather small considering the difference in technology levels.

The Ridgecrest sequence exemplifies how EQN performance can rapidly change due to sudden app adoption. This sequence started with a M6.4 foreshock 36 hours before the mainshock. The foreshock was not detected due to a lack of EQN users in California at the time. However, this foreshock led to EQN installations in sufficient number in the Los Angeles (LA) area (but not in the epicentral region) so that the mainshock was detected in LA, 200 km to the south of its epicenter. Seismic wave propagation times from epicenter to LA where it was detected explains the unusually large detection latency of 40 s (see Supplementary Material). In turn, the mainshock led to new EQN installations at shorter epicentral distances leading to a drop of EQN detection latency to 8 s (median times) for the 27 subsequent detected M2.7 to M4.6 aftershocks (see Supplementary Material).

To evaluate EQN's intrinsic latency, the wave propagation time of the most probable causative seismic phase from the epicenter to the EQN's detection location is subtracted from alert issuance latency. Note that this is an overestimation of cumulative processing and transmission delays as it implicitly assumes that acceleration (i.e., the monitored parameter) peaks at seismic phase onset. This implies that the minimum and median latencies (0.5 s and 4.3 s respectively, Table 1) characterize the best detection latencies that the EQN system can offer. Such fast detection is an achievement considering EQN's low investment cost.

In summary, EQN detection latency with respect to origin times for crustal earthquakes in regions with a significant app audience is comparable (5-8 s) to latencies observed in systems such as ShakeAlert® and, in the best-case scenario, it could be as low as a couple of seconds.

5 EQN warning times

Warning time is defined for a given target intensity as the time delay between the issuance of the alert and when the S-wave arrives at the users' locations who experience that target intensity. Being computed for the slower and stronger S-wave, it assumes that the P-wave is imperceptible and that from a user point of view this is the delay between the alert issuance and the perceived tremor. It assumes that the maximum intensity is generated by the onset of S-wave. Warning times have been computed at target intensities 4 (largely observed), 5 (strong) or 6 (slightly damaging) for all detected earthquakes (without any geographical restrictions) greater than M4.5 in Italy and USA and greater than M5 in the rest of the world. Intensities with respect to radial distance were estimated through intensity predictive equations (IPE) according to the validity domain of the considered IPE. Region-specific IPE have been used in the Western USA (Atkinson et al., 2014), and Italy (Tosi et al., 2015) for crustal earthquakes (focal depth between 0 and 40 km). For all other regions, including deeper earthquakes, the same IPE (Allen et al., 2012) was used. This earthquake dataset being global, for the sake of homogeneity, earthquake parameters are from US Geological Survey (USGS).

According to these estimations, over the 72 detected earthquakes greater than M4.5 or M5, EQN issued early warnings for target intensity 4 for 53 (74%) earthquakes of them (i.e., on average twice a month) located in 11 countries in North, Central and South America, Europe, and Asia (Figure 2 andFigure ***3***). Among these, 18 events also benefited from a warning for target intensity 5 and for two earthquakes there was a warning for target intensity 6: M6.4 November 26th, 2019 Albania and M6.2 July 26th, 2019 Panama. As expected, for a given target intensity, warning times increase with increasing magnitude and for a given earthquake, they decrease with increasing target intensities. For earthquakes greater than M6, estimated warning times are typically more than 10 s for target intensity 4 and more than 5 s for target intensity 5, long enough for the user to take protective measures (Figure 2).

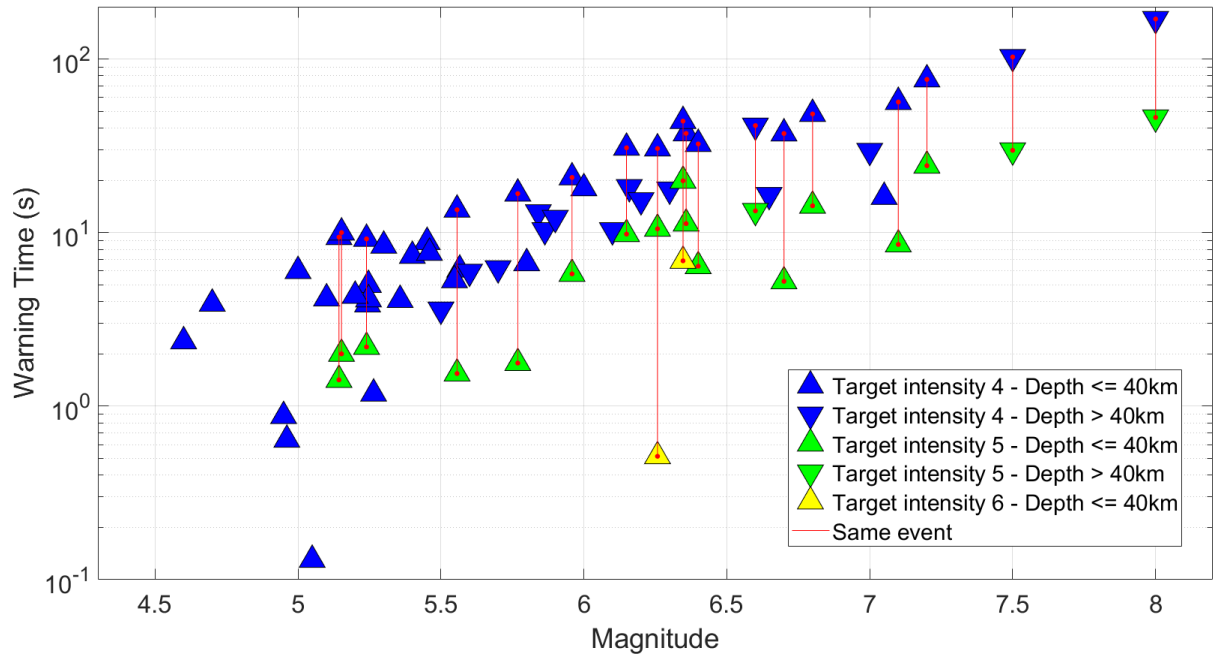

Figure 2. Estimated warning times for the 53 earthquakes detected worldwide with magnitude equal or greater than 4.5 with positive warning time. Blue, green, and yellow triangles depict warning times for target intensities 4, 5, and 6, respectively. Crustal and deep earthquakes are shown by triangles and inverted triangles, respectively. Warning times related to the same event are connected by red lines. For sake of clarity, magnitude is altered by a random shift of +/-(0.03, 0.06) for earthquakes sharing the same magnitude.

The warning time for target intensity 6 for the Panama earthquake is too short for individual protective action. However, for the Albania earthquake, which struck at night and killed 51 people, a warning time of 6.9 s for intensity 6 is estimated through the IPE, for a detection delay of 5.1 s after its occurrence, and a location of the detection 20 km from its epicenter.

According to the IPE, the isoseismal for intensity 6 was at 34 km from epicenter compared to 45 km from the empirical intensity-distance curve derived from about 4,000 eyewitnesses' reports crowdsourced for this event (Bossu et al., 2020). This implies that the warning times derived from the IPE is likely underestimated by about 2 s for intensity 6 leading to a warning time for "slightly damaging" shaking exceeding 8 s. Based on the spatial distribution of EQN users at the

time of the earthquake, and neglecting the transmission delay of the alert, we estimate that 1,005 of them received the early warning for intensity 6, 231 for intensity 5 and 632 for intensity 4. With approximately 800,000 inhabitants within 40 km of the epicenter, the proportion of warned individuals remains small in this case. Still, it proves that EQN can offer significant warning time for damaging shaking levels and so has the potential to lower individual seismic risk for its users.

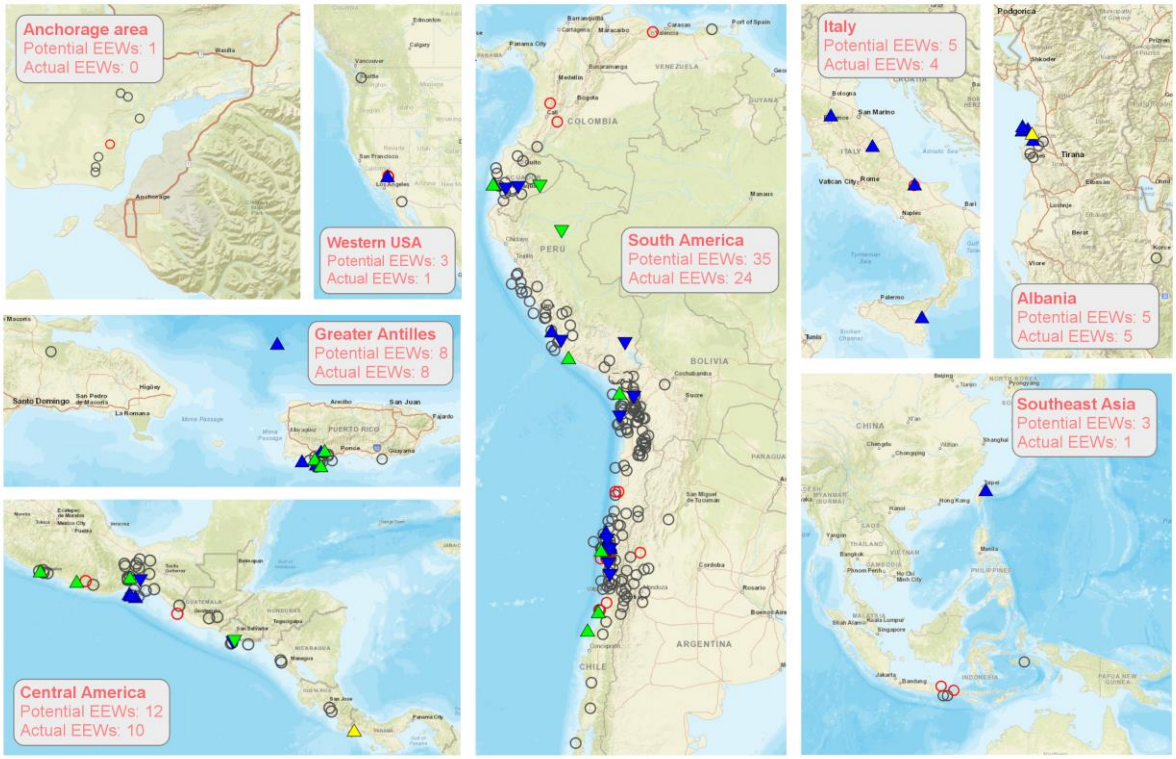

Figure 3. Geographical distribution of the 53 earthquakes for which a positive warning time is determined, shown as triangles (see Figure 2 for legend). All other EQN detected earthquakes of magnitude M4.5 or above are represented by circles, in red when the maximum onshore intensity reached or exceeded intensity 4 (for which an EEW is theoretically possible) and in grey otherwise. The number of EEW in the legends indicates the number of positive warning times at intensity 4.

6 Do EQN users take protective actions after a warning?

The reaction to, and understanding of, early warning has been assessed from an online survey of EQN users in the felt area of the destructive M8 2019 Peru earthquake to evaluate EQN efficiency in terms of individual risk reduction (see Fallau et al., 2021). This earthquake had a focal depth of 120 km and generated two EQN detections, one in Peru and one in Ecuador. Alerts were issued for 599 users for intensity 5 and 54,228 for intensity 4, respectively. The survey was carried out from July 23rd to August 19th, 2019. It was initiated through a message sent for technical reasons to all Spanish language EQN app, linking to an online questionnaire in Spanish. There were 61,863 users within 1,500 km of the epicenter, a distance where USGS and

EMSC estimate the intensity between 3 and 4. 2,719 self-selected participants responded to the questionnaire; ⅔ of them declared to be between 500 to 1,000 km from the epicenter at the time of the earthquake, a range containing the capital cities of Quito and Lima. Most respondents (82%) declared previous earthquake experiences and 25% answered that they had experienced an EQN earthquake early warning before. 72% were convinced or strongly convinced of the usefulness of this app. Among these 2,719 self-selected respondents, 1,704 had the app at the time of the earthquake, while the others installed it following the earthquake. This first group described various experiences: 34% received EQN notification before feeling the shaking as expected from a PEEW system, 34% received it after having felt the shaking, 11% received the notification but did not feel the quake, 14% did not receive the notification while feeling the shaking, and 6% neither received the notification nor felt the quake.

Importantly, among the users who received the notification before feeling the shaking, 79% understood that a tremor was about to hit. This means they had a good comprehension of what an early warning is but when asked about their reaction (several answers possible), only 25% performed “drop, cover and hold”, 10% ran outside, and 3% did nothing. Their priority was to warn relatives nearby (56%) or for the ones not in immediate proximity through social media (23%), and to wait for the shaking (36%).

This single study based on self-selected participants and on a single case shows that a low-cost smartphone based PEEW system can offer an actual early warning to some users even if the alert dissemination delay is unknown and may differ from one user to the next. However, in its current setting, and although the meaning of the notification is often understood, it only leads to adequate protective actions in a minority of cases, possibly because it does not answer an expressed priority need, which is to inform loved ones who may not have the app. The fact that EQN is appreciated by most of its users suggests that, despite EQN’s inability to systematically guarantee an early warning, such a service combining early warning and rapid detection of felt earthquakes is valued by its users and constitutes a progress in public earthquake information.

7 Conclusions

EQN exploits smartphone ubiquity to create an operational network that provides an early warning service to its users. This service differs from conventional services in several aspects as EQN’s alerting strategy is not based on predicted intensity and such predictions are not included in its warning messages. As a consequence, it also provides rapid information for small magnitude felt earthquakes for which no early warning is possible. This also removes errors due to differences between predicted and actual spatial distributions of shaking and bypasses the classic confusion among the public between magnitude and intensity. All of which simplifies the service’s behavior and the content of its warning messages which otherwise can be difficult to understand from a user point of view, especially in a few seconds, as illustrated after the Ridgecrest earthquake where alerting strategy had to be modified following users’ feedback (Allen et al., 2018; Cochran & Husker, 2019). Also, although EQN users are volunteers and so EQN’s alerting strategy has not yet been proven suitable for all audiences, receiving alerts for smaller earthquakes has not been identified by EQN’s users as a weakness, and extending early warning service to also offer rapid public information for felt earthquakes seems generally to be an appreciated feature (Allen et al., 2018). Thus, EQN’s early warning and rapid information services are a significant improvement for seismically active regions of the globe not yet covered by conventional PEEWs.

Acknowledgments

The authors express their thanks to M. Corradini and M. Landès for fruitful discussions, Héctor Massone (CSN) for his identification of additional small magnitude earthquakes in Chile, as well as Eric Calais and Fabrice Cotton for their valuable suggestions for improvement of the manuscript.

This article was partially funded by the European Union's Horizon 2020 Research and Innovation Program under grant agreement RISE No. 821115 and grant agreement TURNKey No. 821046. Opinions expressed in this article solely reflect the authors' views; the EU is not responsible for any use that may be made of information it contains.

Data Availability Statement

Datasets for this research are available in these in-text data citation references: Fallou et al. (2021) and Steed et al. (2021a, 2021b).

References

Allen, R. M., & Melgar, D. (2019). Earthquake early warning: advances, scientific challenges, and societal needs. *Annual Review of Earth and Planetary Sciences*, 47, 361–388. doi:10.1146/annurev-earth-053018-060457

Allen, R. M., Cochran, E. S., Huggins, T. J., Miles, S., & Otegui, D. (2018). Lessons from Mexico's earthquake early warning system. *Eos, Earth and Space Science News*, 99. doi:10.1029/2018EO105095

Allen, T. I., Wald, D. J., & Worden, C. B. (2012). Intensity attenuation for active crustal regions. *Journal of Seismology*, 16(3), 409–433. doi:10.1007/s10950-012-9278-7

Atkinson, G. M., Worden, C. B., & Wald, D. J. (2014). Intensity prediction equations for North America. *Bulletin of the Seismological Society of America*, 104(6), 3084–3093. doi:10.1785/0120140178

Bossu, R., Fallou, L., Landès, M., Roussel, F., Julien-Laferrière, S., Roch, J., & Steed, R. (2020). Rapid public information and situational awareness after the november 26, 2019, Albania earthquake: lessons learned from the LastQuake system. *Frontiers in Earth Science*, 8, 235. doi:10.3389/feart.2020.00235

Chung, A. I., Meier, M. A., Andrews, J., Böse, M., Crowell, B. W., McGuire, J. J., & Smith, D. E. (2020). ShakeAlert earthquake early warning system performance during the 2019 Ridgecrest earthquake sequence. *Bulletin of the Seismological Society of America*, 110(4), 1904-1923. doi.org:10.1785/0120200032

Cochran, E. S., & Husker, A. L. (2019). How low should we go when warning for earthquakes? *Science*, 366(6468), 957–958. doi:10.1126/science.aaz6601

Cremen, G., & Galasso, C. (2020). Earthquake early warning: recent advances and perspectives. *Earth-Science Reviews*, 205, 103184. doi:10.1016/j.earscirev.2020.103184

Fallou, L., Bossu, R., Steed, R., Finazzi, F., & Bondár, I. (2021). A Questionnaire Survey of the Earthquake Network App's Users in Peru Following an M8 Earthquake in 2019. V. 0.9. GFZ Data Services. https://doi.org/10.5880/fidgeo.2021.001 (Preview link: https://dataservices.gfz-potsdam.de/panmetaworks/review/12b6bb5153e39e7ed20dc0bda0d924dd39c60e0376617fb1ab2798cb0f1cb1a8/)

Finazzi, F. (2020). The earthquake network project: a platform for earthquake early warning, rapid impact assessment, and search and rescue. *Frontiers in Earth Science*, 8, 243. doi:10.3389/feart.2020.00243

Finazzi, F., & Fassò, A. (2017). A statistical approach to crowdsourced smartphone-based earthquake early warning systems. *Stochastic Environmental Research and Risk Assessment*, 31(7), 1649–1658. doi:10.1007/s00477-016-1240-8

Kohler, M. D., Cochran, E. S., Given, D., Guiwits, S., Neuhauser, D., Henson, I., et al. (2018). Earthquake early warning ShakeAlert system: west coast wide production prototype. *Seismological Research Letters*, 89(1), 99–107. doi:10.1785/0220170140

Kong, Q., Patel, S., Inbal, A., & Allen, R. M. (2019). Assessing the sensitivity and accuracy of the MyShake smartphone seismic network to detect and characterize earthquakes. *Seismological Research Letters*, 90(5), 1937–1949. doi:10.1785/0220190097

Nakayachi, K., Becker, J. S., Potter, S. H., & Dixon, M. (2019). Residents' reactions to earthquake early warnings in Japan. *Risk Analysis*, 39(8), 1723–1740. doi:10.1111/risa.13306

Steed, R., Bossu, R., Finazzi, F., Bondár, I., & Fallou, L. (2021). Analysis of Detections by the Earthquake Network App between 2017-12-15 and 2020-01-31. V. 0.9. GFZ Data Services. https://doi.org/10.5880/fidgeo.2021.007 (Preview link: https://dataservices.gfz-potsdam.de/panmetaworks/review/9435b0cfcfb380571fe081844f6252c17b756a80a8344045609983874297bd69/)

Steed, R., Bossu, R., Finazzi, F., Bondár, I., & Fallou, L. (2021). Analysis of Strong Motion Waveforms Near the Locations of Detections by the Earthquake Network App in Chile, the USA and Italy. V. 0.9. GFZ Data Services. https://doi.org/10.5880/fidgeo.2021.002 (Preview link: https://dataservices.gfz-potsdam.de/panmetaworks/review/6aa55a072b38fd90bddb0ca01530ce273bc0c1967cdf84c12801a4fb8dfd070c/)

Suárez, G., Novelo, D., & Mansilla, F. E. (2009). Performance evaluation of the seismic alert system (SAS) in Mexico City: a seismological and a social perspective. *Seismological Research Letters*, 80(5), 707–716. doi:10.1785/gssrl.80.5.707

Tosi, P., Sbarra, P., De Rubeis, V., & Ferrari, C. (2015). Macroseismic intensity assessment method for web questionnaires. *Seismological Research Letters*, 86(3), 985–990. doi:10.1785/0220150127

Geophysical Review Letters

Supporting Information for

"Shaking in 5 seconds!" A voluntary smartphone-based earthquake early warning system

Rémy Bossu[1,2], Francesco Finazzi[3], Robert Steed[1], Laure Fallou[1] and István Bondár[4]

1. European-Mediterranean Seismological Centre; Arpajon, France.
2. CEA, DAM, DIF, 91297; Arpajon, France.
3. University of Bergamo, Department of Management, Information and Production Engineering; Dalmine, Italy.
4. ELKH Research Centre for Astronomy and Earth Sciences, Geodetic and Geophysical Institute; Budapest, Hungary.

Contents of this file

Additional Supporting Information (Files uploaded separately)

Introduction

This supporting section describes extra technical details about the operation of the EQN detection network and the analysis of the EQN detections. There are 2 datasets which summarize the results of the analysis and were used to create the graphs and figures in the article. In the following sections these data sets are described, and some extra figures derived from them are presented.

Text S8 briefly describes a comparison of the EQN detections to strong motion waveforms that was carried out to demonstrate that the EQN detections in the analysis were strongly correlated with ground shaking in every case where they could be associated to an earthquake.

Text S1. Detection Methodology

The EQN app begins to monitor the smartphone's internal accelerometer when the phone is charging and not systematically moving (e.g., being transported) and 2-15 min after the phone's screen has been inactivated.

The app records the acceleration of the device in batches of data of 3 s at the highest allowed frequency (typically 50-100 Hz) and then calculates the variance. The app monitors for changes in variance compared to each smartphone's background variance using a standard control chart technique (s-type control chart). If a vibration is detected, then a trigger is sent to the EQN server in Europe with the location of the phone found via the Android or iOS Location API. It also sends the maximum acceleration seen during the triggering section of the waveform and the delay caused by the analysis of the waveform in milliseconds. However, the starting time of the vibration within the waveform section is not analyzed meaning that the time recorded after each trigger will be 0-3 s after the start of strong motion. Since the EQN app collection windows are not synchronized, if the density of recording EQN apps is high enough, then some smartphones will trigger before the others even if they record identical strong motions. There is an additional delay due to the latency of the internet which is unknown but is estimated to be less than 300 ms and probably less than 100 ms, but occasionally it might be larger than 1 s in less developed countries or remote regions with respect to Europe.

Each smartphone sends on average around 30 triggers signals per day that are not related to earthquakes. Anything that knocks or shakes the phone while it is recording, such as its owner or another app's notification could cause one of these false triggers. So, earthquake detection relies on there being an aggregate of triggers that are localized within the same region. For each trigger arriving at the server, the number of triggers within a 0.3 deg radius (~33 km) and 30 s of the trigger are counted. The number of active EQN apps is also counted within this region. Detection occurs if the following parameter is large enough:

$$S = N_{\varepsilon}/\varepsilon\lambda - 1, \quad (S1)$$

where N_{ε} is the number of triggers seen during a $\varepsilon=30$ second period, and

$$\lambda = \exp(\beta_0 + \beta_1 \nu_t), \quad (S2)$$

where ν_t is the number of active EQN apps at the moment of detection while β_0 and β_1 are tuning parameters. Detections occur when $S>h$ where h is a threshold that varies by region and is calculated so that, on average, there is only one false detection per year per country (8).

Detections are automatically eliminated if the maximum acceleration recorded is very high for 10% of the triggers. These high accelerations are usually caused by phones vibrating due to notifications from other apps. EQN can also make false detections due to strong thunderstorms and so an online service is used to reject detections coincident with such storms.
Once a detection occurs, any subsequent detection within 300 km and 2 min of the first is automatically suppressed.

Text S2. Earthquake Notifications

It is equally important to rapidly disseminate an earthquake warning as it is to detect it. When a detection occurs, users within a certain distance of the detection are sent an alert that makes a sound on the user's smartphone and shows an estimated countdown to the arrival of the S wave. By default, this distance is 300 km, but users can configure the distance up to which they will receive the alert. They can also decide whether they will receive any alerts and what sound they will make. The EQN detection location and time are taken as a proxy for the earthquake's epicenter and origin time in order to make the S wave arrival calculation.

EQN uses the Firebase notification service (https://firebase.google.com/) for alerts. The notifications are sent in order of increasing distance from the epicenter in order to maximize the chance of providing early warning. Although the actual delay between EQN's servers requesting an alert and the users' smartphones responding is hard to ascertain due to technicalities, qualitative feedback via EQN's user forums suggests that the average delay is likely to be a few seconds at most.
As described in the main article, a secondary alert can be triggered by users making reports of shaking via the app. As for the primary alert, users can customize how they receive these alerts and at what distance from the detection location.

Text S3. Analysis of EQN detections

The events detected by the Earthquake Network (EQN) app between Dec. 15th, 2017 and Jan. 31st, 2020 were the focus of this article's analysis. This time range was chosen so that EQN's detection procedures would be stable during the entire period. There were 1792 detections during this period in 19 countries. In order to perform quantitative analysis, 2 sub-datasets were extracted from this global dataset:

- Data S1 - restricted to the 550 detections detected in Chile, USA, and Italy.
- Data S2 - restricted to the 134 detections that could be associated to earthquakes in the USGS catalogue ≥ M4.5 in Italy and USA and ≥ M5 in the rest of the world.

There are 68 detections that are common to both datasets.

From the countries with a strong user base of the app, we chose to analyze events in Chile, USA, and Italy due to the accuracy and completeness of their catalogues. They also have moderate-high seismicity, with a broad range of magnitudes from small events

to occasionally large, devastating earthquakes. Importantly, all three regions operate dense seismological station networks that are able to produce accurate event locations and magnitude estimates. An epicentral location inaccuracy of 15 km translates to a seismic phase arrival time change of 2-3 s which can become important in the case of EQN due to its rapid response. All 3 regions also have dense accelerometer networks whose records were used to validate the EQN triggers.

The second dataset contains EQN detections from around the world as long as they could be associated to earthquakes with magnitudes greater or equal than M5 - or greater or equal than M4.5 in the USA and Italy. This dataset was used to analyze the degree to which EQN offers early warning of earthquakes to its users (see Figure 3). There were also 3 earthquakes that were detected twice by EQN, normally such duplicate detections are suppressed automatically but all 3 earthquakes were large magnitude events (M7.0, M7.5 and M8.0) that led to EQN making detections at distances far from the epicenters. These 3 duplicate detections have been removed from the dataset for clarity.

These datasets are included in the supplementary material as Data S1 and Data S2 and are also available from an external data repository (Steed et al., 2021). The fields of the datasets are described in Table S1. The USGS and INGV catalogues of earthquake parameters were searched via FDSN requests while the CSN catalogue was provided upon request. Calculations of the P and S seismic phases used the ak135 model and were carried out by the obspy Python library (see following sections for other calculation of other fields).

We can see the distribution of magnitudes in Data S1 in Figure S3 and a histogram of detection dates in Figure S4.

Text S4. Association of Detections with Earthquakes

For the purposes of the analysis, it is important to associate each EQN detection with earthquakes parameters held in an institute's catalogues of events. The following procedure was used for association:

1. Earthquakes were selected from the catalogue from 250 s before the time of the detection until 4 s afterwards.
2. Earthquakes were selected that are also within the association distance defined by each earthquake's magnitude (see Figure S2).
3. For each earthquake, the arrival time of the P waves at the EQN detection location was estimated using the ak135 model's speed of 8.04 km/s. The events whose P waves arrive within 90 s before the EQN detection and 10 s after the detection were chosen.
4. If multiple earthquakes remained in the selection, then the earthquake of the largest magnitude was chosen as the associated earthquake.

Out of the 550 detections in Data S1, 539 could be associated with earthquakes from the available catalogues. 519 detections matched to a single earthquake, 14 matched to 2 earthquakes, 6 to 3 detections and 11 matched to no earthquakes. Manual investigation

of the 11 unexplained detections led to 4 additional events that could be associated with earthquakes (see main article text).

Text S5. Causal Seismic Phase of EQN detections

It has been found that EQN detections can be triggered by either P or S seismic phases, see Figure S5. The EQN detections were split heuristically into being caused by P or S phases using the criteria:

Caused by S if (detection delay w.r.t. S > 0 s) & (detection delay w.r.t. P > 6 s). (S3)

Note that distinguishing between P and S phases is less clear within 50 km of the epicenter since both arrive within a short interval of time. In addition, the EQN detections are triggered by strong motion due to the relative insensitivity of the smartphone accelerometers and the P/S phase arrival does not exactly coincide with the onset of motion strong enough to cause a detection.

Text S6. Calculation of Shaking Intensities

Intensity predictive equations (IPE) were used to create the columns in the datasets (Data S1 and S2) and for the analysis of early warning times presented in the article. An IPE predicts the total felt intensity of shaking with respect to hypocentral distance for a given magnitude of earthquake. For a given delay from the origin time of an earthquake, the distance of the S phase from the epicenter can be calculated using the ak135 model and the intensity of shaking for this distance can then be calculated using the IPE. Alternatively, the distance at which the intensity reaches a certain value can be found and then the time at which the S phase passes this distance can be calculated in order to estimate whether there would be time for a warning to be given to people at this intensity.

To convert between hypocentral and epicentral distance:

$$r^2 = d^2 + 4R(R-d)\sin^2(s/2R), \quad (S4)$$

where r is the distance from the hypocentral, d is the hypocentral depth, R is the Earth's radius and s is the epicentral distance.

For most earthquakes, the IPE from Allen et al. 2012 were used, this formula is only valid for magnitudes >M5 and so we restricted the analysis accordingly.

If r < 50 km

$$\text{Intensity} = 2.085 + 1.428M + 1.402\ln\sqrt{(r^2 + R_m^2)} \quad (S5)$$

else

$$\text{Intensity} = 2.085 + 1.428M + 1.402\ln(\sqrt{(r^2 + R_m^2)}) + 0.078\ln(r/50), \quad (S6)$$

where r is the hypocentral distance, M is the magnitude of the earthquake and

$$R_m = -0.209 + 2.042\exp(M-5). \quad \text{(S7)}$$

For the Italian earthquakes, the IPE from Tosi et al. 2015 was employed for crustal earthquakes (focal depth between 0 and 40 km):

$$\text{Intensity} = -2.15 \log_{10}(r) + 1.03M + 2.31. \quad \text{(S8)}$$

For the western USA, the IPE from Atkinson et al. 2014 was used:

$$\text{Intensity} = 0.309 + 1.864M - 1.672\log_{10}(\sqrt{(r^2 + 14^2)}) - 0.00219\sqrt{(r^2 + 14^2)} + 1.77\max(0, \log_{10}(r/50)) - 0.383M \log_{10}(\sqrt{(r^2 + 14^2)}). \quad \text{(S9)}.$$

Text S7. Detection rates during day and night

The EQN's network of sensors is dependent upon the number of smartphones with the app that are plugged in and charging, intuitively it is expected that the density of the network will increase during the nighttime since many people charge their phones overnight while they sleep. It may also be that there is a lower background of vibrational noise during the night. For the analysis, nighttime was defined as between 23:00 and 07:00 local time. This means there are 16 hours of day and 8 hours of night and so a factor of 2 is needed to compare rates. The rate of detection was indeed found to be higher during the night by a ratio of 3.1 for Data S1 (see Table 1).

Text S8. Comparisons with Strong Motion Waveforms

For Data S1 (detections in Chile, USA, and Italy), a search was made using the FDSN protocol for accelerometer station waveforms within 20 km of each EQN detection. The waveforms were detrended, calibrated as acceleration measurements and bandpass filtered between 0.5-12 Hz. The waveform was also shifted in time to account for the difference in radial distance for the EQN detection location and the strong motion station with respect to the epicenter of the earthquake. The shift crudely assumed a seismic phase velocity of 8 km/s and the time shift was less than 1s in the majority of cases. The correction ensured that there was no confusion in causality for the analysis whereby the EQN detection occurred before the strong motion arrived.

Accelerometric data was found for 410 of the 550 detections in Data S1. The analysis demonstrated a strong correlation between strong motion and the EQN detections as would be expected and that it was also found that even small accelerations were able to cause EQN triggers (see Figure S6). The analysis also corroborated that the detections can be triggered by both P and S seismic phases (see also Figure S5 which shows this through a timing analysis) although it should be remembered that strong motion necessary to cause triggers might follow a few seconds after the passing wavefront.

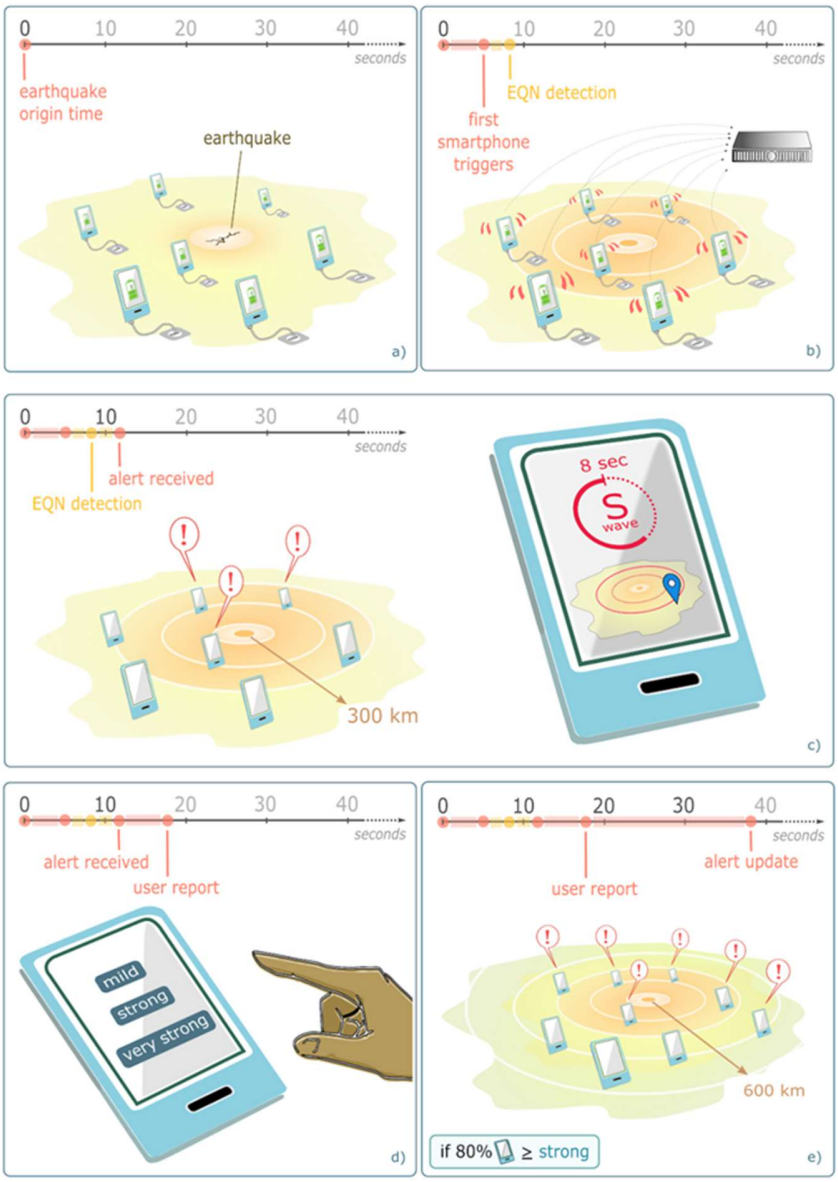

Figure S1. The EQN app utilizes a charging smartphone as a ground motion detector. Earthquakes are detected through a cluster of smartphone triggers. Once detected, an alert is issued to all users within a default distance of the detection and displays a countdown of the estimated S-wave arrival time at the user's location. Users can qualitatively report the level of shaking if they choose to. If most of them reports strong shaking, a second alert is issued in an extended distance. Epicenter location is published on EQN app once available.

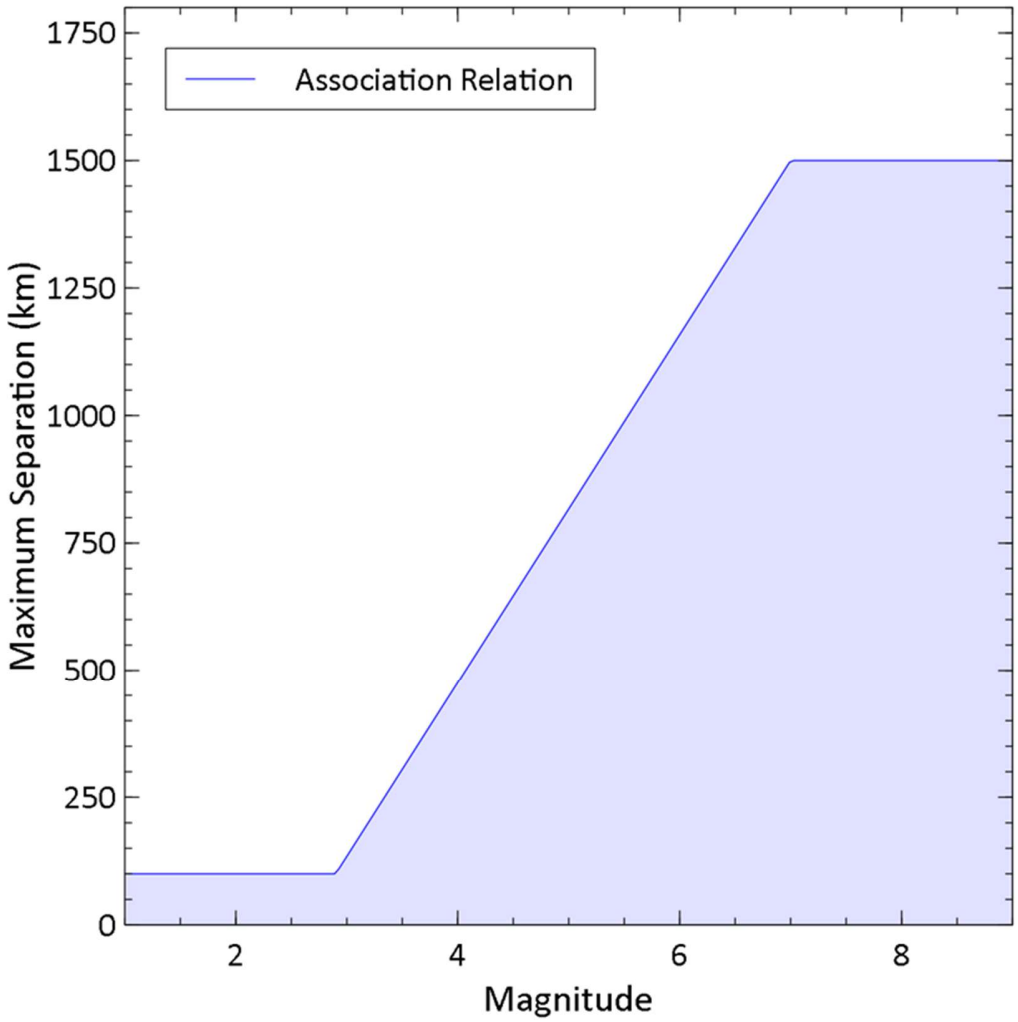

Figure S2. Association between an earthquake and EQN detection is allowed only if the separation between the epicenter and the EQN detection location is less than a threshold distance dependent upon the earthquake's magnitude as shown above.

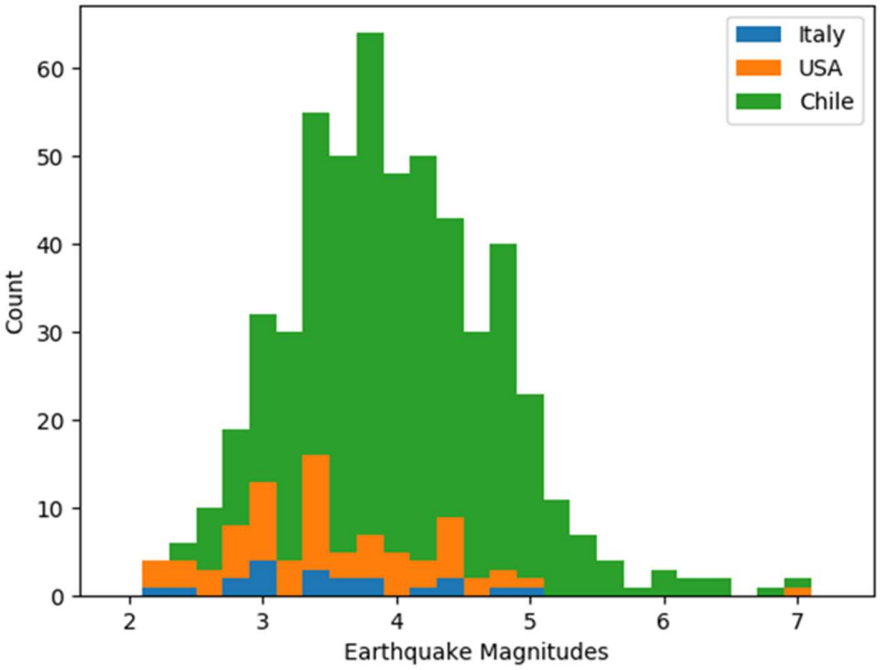

Figure S3. This stacked Histogram shows that EQN detected earthquakes over a range of magnitudes in Chile, USA, and Italy. 539 out of the 550 EQN detections studied were associated with earthquakes with published parameters.

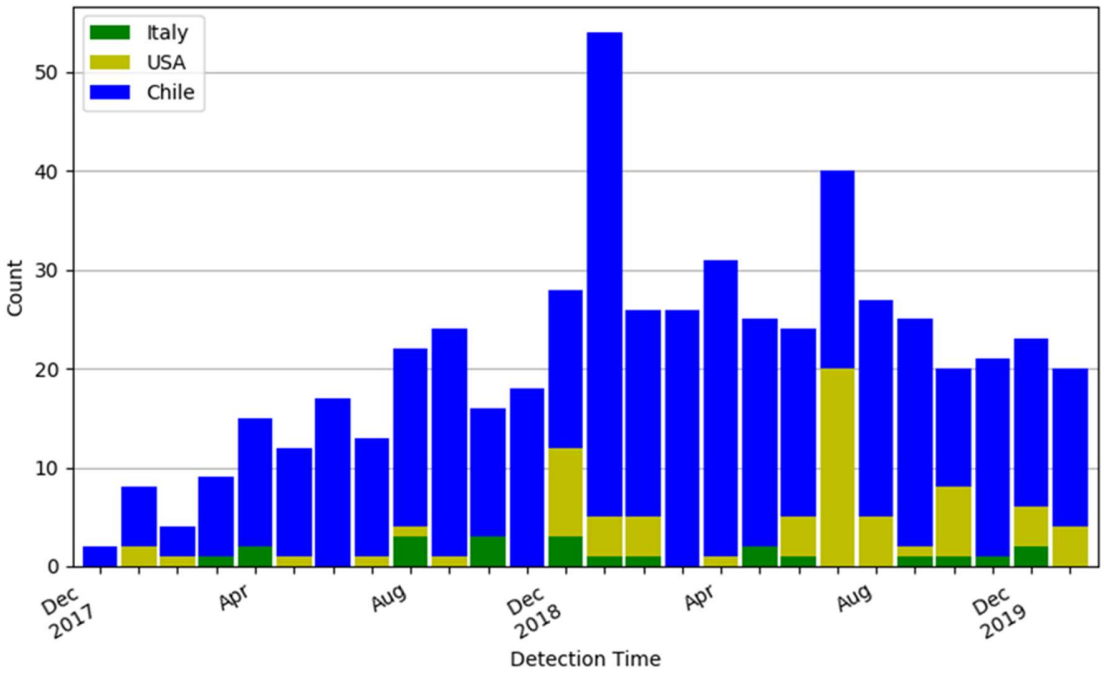

Figure S4. A stacked histogram of the number of EQN detections per month in Chile, USA, and Italy. A growth in the number of directions can be seen for Chile and the USA over this period.

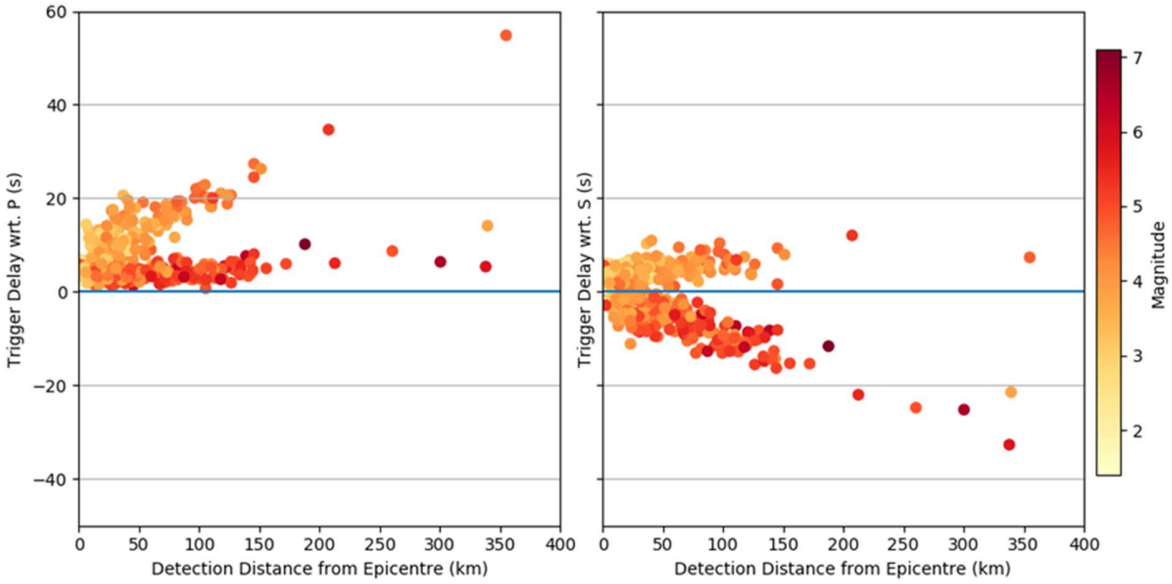

Figure S5. Determination of whether EQN detections follow the P or S seismic phase using Data S1. (550 detections in Chile, USA, and Italy). The arrival of the P and S phases at the detection location were calculated using the ak135 model and the latency between each phase arrival and the detection time is plotted against separation between the detection location and the epicenter. It can be seen that detections closely follow the passing of either the P or S phases and that EQN tends to detect larger magnitude earthquakes using the P wave.

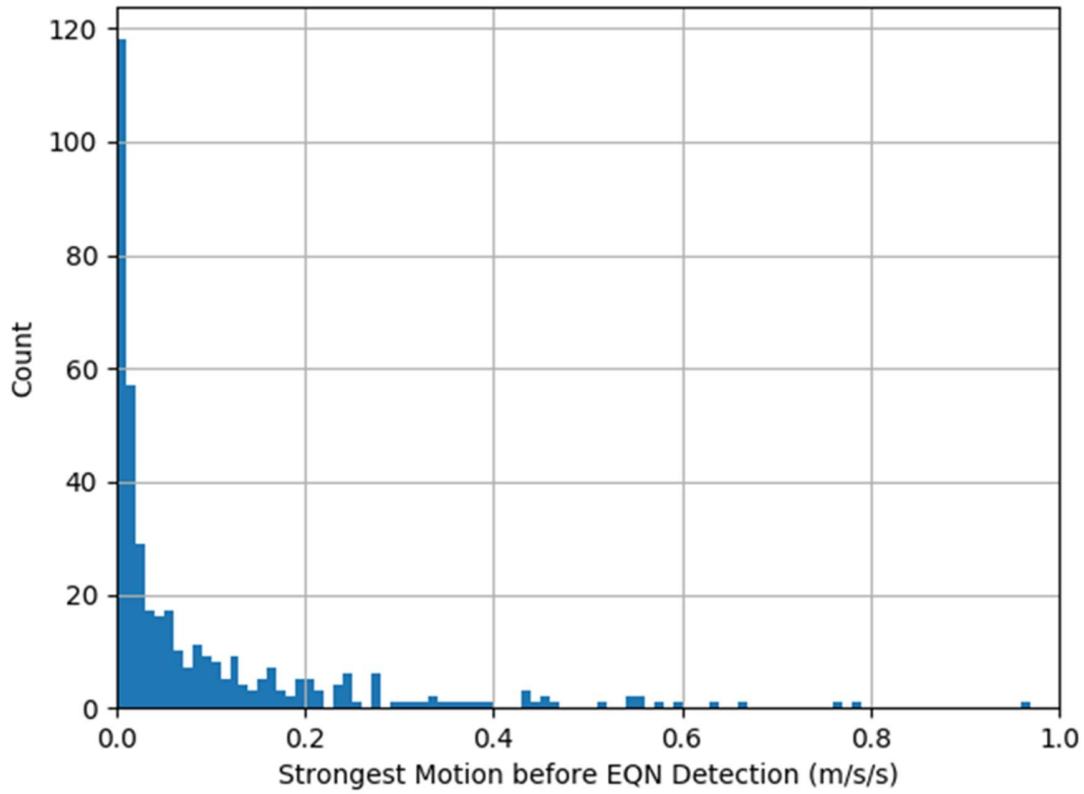

Figure S6. Histogram of the strongest acceleration found in the closest strong motion recording for each EQN detection in the 30 s period before detection. The results are only approximate since the level of shaking can vary dramatically even over a distance of 10-20 km due to local site effects.

Field	Description
peakid	Each EQN detection has a random 7-digit numeric id associated.
det_lat	Latitude where EQN detection occurred (degrees).
det_lon	Longitude where EQN detection occurred (degrees).
country	Country iso3166 code, one of {'chl','usa','ita'}.
detectiontime	Date and time of EQN detection (Iso8166 format) (UTC time zone).
detectiontime_local	Localized date and time of EQN detection.
pytz	Time zone of EQN detection.
nighttime	Did EQN detection occur between 23h and 7h local time? (Boolean)
signals	The number of signals that caused the EQN detection to trigger.
actives	The number of active EQN apps within 30 km of the detection location.
felt_reports_green	Number of felt reports collected indicating 'green' within 3 min from detection and within a radius of 300 km.
felt_reports_yellow	Number of felt reports collected indicating 'yellow' within 3 min from detection and within a radius of 300 km.
felt_reports_red	Number of felt reports collected indicating 'red' within 3 min from detection and within a radius of 300 km.
notification_time	When the notification based on felt reports was sent to the Firebase notification service.
notification_delay_from_detection	Delay between detection and the notification.
Intensity_strong	If 1, a second alert for strong earthquakes was sent. The time of this second alert is the same of notification time since it is based on the felt reports.
cat	Seismic catalogue used for earthquake parameters.
num_eq_matches	Number of potentially associated earthquakes in catalogue.
origintime	Date and time of associated earthquake in catalogue (UTC).
magtype	Type of magnitude for associated earthquake.
magnitude	Magnitude of associated earthquake in catalogue.
eq_lat	Latitude of associated earthquake in catalogue (deg).
eq_lon	Longitude of associated earthquake in catalogue (deg).
depth	Depth of associated earthquake in catalogue (km).
separation	Separation of EQN detection from epicenter of associated parameters.
detectiondelay	Delay between origin time and EQN detection (s).
P_at_surface_delay	Delay for P wave to reach the Earth's surface (s).
offshore	Was earthquake offshore? (Boolean).
dist_shore	Distance from epicenter to closest point on the shore (km).
closest_land_lat	Latitude of point of coast closest to the epicenter (deg).
closest_land_lon	Longitude of point of coast closest to the epicenter (deg).
P_at_coast_delay	Delay for P wave to reach the closest point on the coastline (and at the surface) (s).
P_on_land_surface_delay	Delay for the P wave to read the surface (or the coast if applicable) (s).
detectiondelay_wrt_P	Delay between the P wave arriving at the EQN detection location and the detection time (s).
detectiondelay_wrt_S	Delay between the S wave arriving at the EQN detection location and the detection time (s).
causal_phase	Whether the EQN detection was estimated to have been caused by the P wave or the S wave.
intensity_at_0ld	The predicted intensity of the earthquake for the location of the S wave at the moment of the EQN detection.

intensity_at_5ld	The predicted intensity of the earthquake at locations with a lead time of 5 s with respect to the S wave at the moment of the EQN detection.
intensity_at_10ld	The predicted intensity of the earthquake at locations with a lead time of 10 s with respect to the S wave at the moment of the EQN detection.
intensity_at_15ld	The predicted intensity of the earthquake at locations with a lead time of 15 s with respect to the S wave at the moment of the EQN detection.
sm_net	The seismic network if strong motion accelerometer data was found nearby.
sm_sta	The station name if strong motion accelerometer data was found nearby.
sm_loc	The separation between the strong motion station and the EQN station (km).
sm_unit	One of {'acc','vel','disp'} where acc is acceleration (m/s/s), vel is velocity (m/s) and disp is displacement (m).
sm_sta_lat	Latitude of strong motion station (deg).
sm_sta_lon	Longitude of strong motion station (deg).
sm_sta_elv	Elevation of strong motion station (m).
sm_sep_eqn_sta	Separation between EQN detection and strong motion station (km).
sm_strongest_motion	Strongest value recorded by station.
sm_strong_motion_time	Time of strongest motion (this already accounts for sm_dt_correction).
sm_strongest_motion_ eqn_delay	Delay between strong motion and EQN detection (this already accounts for sm_dt_correction).
sm_dt_correction	Time correction (s) due to difference in distances of station and EQN detection from the epicenter. A velocity of 8 km/s is used to convert between distance and time.

Table S1. A description of the fields in the Data S1 & Data S2 datasets. Although the S2 dataset does not contain the final 16 fields.

Magnitude	Origin time	ShakeAlert® detection delay (s)	EQN detection delay (s)	EQN detection distance (km)
3.9	2019-12-21 08:24:32.6	6.8	10.4	20
3.8	2019-12-05 08:55:31.65	5.7	5.4	10
4.5	2019-10-15 05:33:42.81	5.6	7.2	3
7.1	2019-07-06 03:19:53.04	6.9	40.0	188

Table S2. Detection latencies for the 4 earthquakes detected by both ShakeAlert® and EQN. These 4 earthquakes were detected in California. They followed the M 7.1 Ridgecrest mainshock. ShakeAlert® detection times were retrieved from Chung et al. (15) for the M7.1 Ridgecrest earthquake in California and from http://earthquake.usgs.gov for the others.

Data Set S1. The 550 EQN detections between Dec. 15th, 2017 and Jan. 31st, 2020 that occurred in Chile, USA, and Italy. The columns of the dataset are described in Table S1.

Data Set S2. The 134 EQN detections from 19 countries between Dec. 15th, 2017 and Jan. 31st, 2020 that have been associated to earthquakes with magnitude greater than M4.5 using the USGS's parameter catalogue. There is overlap with Data S1 with 68 of the detections in both datasets, although different earthquake parameters will have been used for some of those detections in S1.